

# SEGUE-2 Limits on Metal-Rich Old-Population Hypervelocity Stars In the Galactic Halo

Juna A. Kollmeier<sup>1</sup>, Andrew Gould<sup>2</sup>, Constance Rockosi<sup>3</sup>, Timothy C. Beers<sup>4</sup>, Gillian Knapp<sup>5</sup>, Jennifer A. Johnson<sup>2</sup>, Heather Morrison<sup>6</sup>, Paul Harding<sup>6</sup>, Young Sun Lee<sup>4</sup>, Benjamin A. Weaver<sup>7</sup>, and the SEGUE-2 Collaboration

## ABSTRACT

We present new limits on the ejection of metal-rich old-population hypervelocity stars from the Galactic center (GC) as probed by the SEGUE-2 survey. Our limits are a factor of 3-10 more stringent than previously reported, depending on stellar type. Compared to the known population of B-star ejectees, there can be no more than 30 times more metal-rich old-population F/G stars ejected from the GC. Because B stars comprise a tiny fraction of a normal stellar population, this places significant limits on a combination of the GC mass function and the ejection mechanism for hypervelocity stars. In the presence of a normal GC mass function, our results require an ejection mechanism that is about 5.5 times more efficient at ejecting B-stars compared to low-mass F/G stars.

## 1. Introduction

Hypervelocity stars (HVS) have emerged as a promising way to probe the dynamics and physical conditions at the Galactic center (GC). Thus far, the discoveries of HVS have predominantly been B-stars, with the more recent addition of a small number of A-stars

---

<sup>1</sup>Observatories of the Carnegie Institution of Washington, 813 Santa Barbara Street, Pasadena, CA 91101

<sup>2</sup>The Ohio State University, 4055 McPherson Labs, Columbus, OH, 43210

<sup>3</sup>Department of Astronomy and Astrophysics, University of California Santa Cruz, 201 Interdisciplinary Sciences Building (ISB) Santa Cruz, CA 95064

<sup>4</sup>Department of Physics & Astronomy; CSCE:Center for the Study of Cosmic Evolution and JINA: Joint Institute for Nuclear Astrophysics, Michigan State University, E. Lansing, MI 48824 USA

<sup>5</sup>Department of Astrophysical Sciences, Princeton University, Peyton Hall, Princeton, NJ 08544

<sup>6</sup>Department of Astronomy, Case Western Reserve University, 10900 Euclid Ave, Cleveland, Ohio 44106

<sup>7</sup>Center for Cosmology and Particle Physics, New York University, New York, NY 10003

(Brown et al. 2005; Edelmann et al. 2005; Hirsch et al. 2005; Brown et al. 2007a,b, 2009). These objects have been detected at large distances from the GC ( $\sim 70$  kpc); their flight times and spectral types are consistent with ages of less than 100-200 Myr. Empirically, the known HVS constitute a relatively young population. While the youth of this population may reflect a top-heavy mass function at the GC or an ejection mechanism that greatly prefers stars of this mass range, it is also possible that the increased difficulty of locating old-population<sup>1</sup> HVS among a predominantly old halo population has distorted our picture of the conditions at the GC. In the absence of a complete kinematic census of the Galactic halo, it is substantially more difficult to find old-population HVS compared to young-population HVS. This is because the Galactic halo is composed of primarily old-population stars whose red colors are very similar to those of low-mass HVS, which make photometric pre-selection for spectroscopy non-trivial (Kollmeier & Gould 2007). By contrast, there are very few blue stars in the halo, just a handful that are blue due to their youth (such as “runaway B stars”) and not many more old stars (like blue-horizontal branch stars) that live in the halo “legitimately”. Early type stars are more luminous and can be seen to larger distances, and thereby probe larger volumes, relative to the more typical G-stars that predominate in a normal mass function. These factors combine to make the photometric background of non-HVS to HVS significantly reduced for early-type stars. However, regardless of the practical difficulties, it is essential to find the old-population HVS (or determine that they do not exist) if one is to understand the physics at the GC (Kollmeier & Gould 2007). The power of the wide-field spectroscopic capability of the 2nd Sloan Extension for Galactic Understanding and Exploration (SEGUE-2) can be directly brought to bear on this problem.

In a previous paper, we used the entire available Sloan Digital Sky Survey (SDSS) stellar database to place limits on the ejection of metal-rich old-population hypervelocity stars (Kollmeier et al. 2009, hereafter K09). Using turnoff stars collected in SDSS throughout the lifetime of the survey, we analyzed the high-velocity,  $|V_G| > 300 \text{ km s}^{-1}$ , distribution of stars. The underlying sample contained nearly 300,000 stars — a motley collection of calibration stars, failed quasar targets, and fiber-fill. The sheer number of targets allowed us to obtain upper limits to the total ejection rate of  $\Gamma^F < 60 \text{ Myr}^{-1}$  and  $\Gamma^G < 300 \text{ Myr}^{-1}$  for unbound F and G stars, respectively. Comparing to estimates of the B-star ejection rate from the Brown et al. (2007b) survey, we obtained a relative ejection rate of old to young metal-rich HVS consistent with a normal stellar mass function. To probe more deeply into this putative population, we have implemented a well-defined target selection algorithm within SEGUE-2 to more cleanly search for metal-rich old-population HVS that have been ejected from the

---

<sup>1</sup> We use the term “old” as a short-hand for “long-lived”. Similarly, “young” is used to denote “short-lived” stars.

GC.

In Section 2, we describe SDSS, SEGUE, SEGUE-2, and our target selection. In Section 3 we present the results of this selection and derive our sensitivity to metal-rich old-population HVS from which our new limits for the ejection of this population are derived. In Section 4 we discuss these limits.

## 2. Sample

The sample we analyze here comprises a subset of objects targeted within the SEGUE-2 survey.

### 2.1. SDSS, SEGUE and SEGUE-2

SDSS-I was an imaging and spectroscopic survey that began routine operations in April 2000, and continued through June 2005 (Fukugita et al. 1996; Gunn et al. 1998; York et al. 2000; Hogg et al. 2001; Lupton et al. 2001; Smith et al. 2002; Stoughton et al. 2002; Ivezić et al. 2004; Gunn et al. 2006; Tucker et al. 2006). The SDSS and its extensions used a dedicated 2.5m telescope (Gunn et al. 2006) located at the Apache Point Observatory in New Mexico. The Sloan Extension for Galactic Understanding and Exploration (SEGUE) is one of the three key projects in the recently completed first extension of the Sloan Digital Sky Survey, known collectively as SDSS-II. The SEGUE program, which ran from July 2005 to July 2008, obtained *ugriz* imaging of approximately 3500 deg<sup>2</sup> of sky outside of the SDSS-I footprint, with special attention being given to scans of lower Galactic latitudes ( $|b| < 35^\circ$ ) in order to better probe the disk/halo interface of the Milky Way. SEGUE obtained approximately 240,000 medium-resolution spectra of Galactic stars, selected to explore the nature of stellar populations from 0.5 kpc to 100 kpc (Yanny et al. 2009). SDSS-III, which is presently underway, has already completed the sub-survey SEGUE-2, an extension primarily intended to obtain stellar spectra for distant stars that are likely to be members of the outer Galactic halo.

The first seven public data releases from SDSS (Abazajian et al. 2003, 2004, 2005, 2009; Adelman-McCarthy et al. 2006, 2007, 2008) have produced over 350,000 stellar spectra (and their derived atmospheric parameters, where possible). More than 120,000 stellar spectra obtained during the course of SEGUE-2 will be distributed as part of the next public data release, DR8.

The SEGUE Stellar Parameter Pipeline processes the wavelength- and flux-calibrated

spectra generated by the standard SDSS spectroscopic reduction pipeline (Stoughton et al. 2002), obtains equivalent widths and/or line indices for more than 80 atomic and molecular absorption lines, and estimates radial velocities,  $T_{\text{eff}}$ ,  $\log g$ , and  $[\text{Fe}/\text{H}]$  through the application of a number of approaches (Allende-Prieto et al. 2008; Lee et al. 2008a,b). The spectral resolution of the survey is  $R \sim 2000$  over wavelengths 385-920 nm, yielding typical velocity errors of 4-10  $\text{km s}^{-1}$ .

## 2.2. Target Selection

While the target selection method advocated by Kollmeier & Gould (2007) is relatively complete, it would require many fibers on each SEGUE-2 plate. To achieve greater economy of fibers, we adopted the following rather stringent selection for HVS candidates in SEGUE-2. The new selection criteria make use of proper motion information as well as photometric metallicity information to pre-select stars that have enhanced likelihood of being GC ejectees. This experiment, designed to locate the “metal-rich contaminant” to the Galactic halo originally envisioned by Hills (1988), selects stars to have a high probability of being high-metallicity, and to have proper motions consistent with high space velocities from the GC. We select stars satisfying the following criteria:

- 0)  $|b| > 30^\circ$
- I)  $17 < g_0 < 20$
- II)  $\mu > 8 \text{ mas yr}^{-1}$
- III)  $v_{\text{tot}} > 400 \text{ km s}^{-1}$
- IV) either
  - IVa)  $\mu_{\perp} < 6 \text{ mas yr}^{-1}$  or
  - IVb)  $v_{\perp} > 400 \text{ km s}^{-1}$
- V) either
  - Va)  $(0.35 < (g - r)_0 \leq 0.40) \cap (0.375 < (u - g)_0 - 2.5(g - r)_0 < 0.525)$  or
  - Vb)  $(0.40 < (g - r)_0 \leq 0.60) \cap (0.225 < (u - g)_0 - 2.5(g - r)_0 < 0.425)$

where  $\mu$  is the total proper motion as determined by SDSS and USNO-B (Gould & Kollmeier 2004; Munn et al. 2004),  $\mu_{\perp}$  is the component of proper motion perpendicular to the direction

from the GC to the star,  $v_{\text{tot}}$  is the total (3D) velocity (assuming that the star is on a radial orbit), and  $v_{\perp} = \mu d$  is the transverse velocity assuming that the measured proper motion is correct (velocities quoted here are Galactocentric). There are several other criteria that are applied to all SEGUE-2 targets involving proper motions that are designed to remove poorly measured objects due to errors in USNO-B. These are described in greater detail below. However, the crucial point at this stage is that these criteria lead to a dramatic increase in rejected targets for  $|b| < 30$ , which is what motivates Criterion (0).

Criterion (I) restricts the sample to stars with modest  $u$ -band photometric errors. Criterion (II) eliminates many stars, while preserving most HVS. Given the  $4 \text{ mas yr}^{-1}$  errors, criterion (III) eliminates a large fraction of stars surviving (II) while only eliminating 7% of HVS. Criterion (IV) ensures a minimum velocity in a direction consistent with an origin at the GC. Criterion (V) is the most important. It eliminates the overwhelming majority of halo stars and selects for metal-rich stars. The color index  $(u - g)_0 - 2.5(g - r)_0$  “typically” (i.e., at  $g = 19.4$ ) has errors of 0.105 mag, which means that if the color-color relation (see Fig 1) is within a few hundredths of a magnitude of the threshold, then roughly half of the stars will survive this cut. Because of the relatively large error in this index, it is essential to keep the boundary away from the bulk of the metal-poor population, if one wants to avoid massive contamination. Hence, the combination of large errors and requirement of avoiding contamination dictates a color-color cut that will eliminate about half the HVS.

We individually inspected a 20% random sample of the HVS targets rejected by the SEGUE-2 proper-motion selection algorithm on digitized POSS-I and POSS-II plates. We found that essentially all of those rejected because they had less than 4 astrometric epochs were, in fact, spurious targets: they had nearby ( $\lesssim 5''$ ) neighbors that were blended in POSS-I, thus corrupting the proper-motion measurements. Of the rejected targets that passed this test, almost none had any recognizable problem. These constitute 11% of all targets (excluding those rejected for too-few epochs). In addition, we estimate that  $\lesssim 2\%$  of HVS (i.e., random field stars) would have a close neighbor that would lead to rejection as above. Hence, we apply a 0.87 ( $= 1 - 0.11 - 0.02$ ) correction factor to our completeness, due to SEGUE-2 proper-motion selection.

Our color selection is motivated by the requirement that we use minimal fibers per plate, so as not to interfere with any other program (of which there are many; Yanny et al. 2009). To assess the quality of our photometric pre-selection we rely on guidance from the theoretical isochrones computed by An et al. (2009). Figure 1 shows several tracks of stars plotted in color-magnitude and color-color space at several ages for a solar metallicity isochrone and a super-solar isochrone. As can be seen from the figure, our selection recovers solar metallicity objects very well for colors  $0.4 < (g - r)_0 < 0.5$ . At redder colors, the

isochrones formally fall below our selection, but by an amount that is smaller than the color-index error. At bluer colors, we retain substantial sensitivity only to stars above the main-sequence turnoff. For higher-metallicity stars, the isochrones shift upward in the color-index panels, improving our sensitivity at all colors. We are therefore sensitive to solar and super-solar metallicity ejectees. These curves shift downward at lower metallicity (not shown) away from our color-index selection region, and we lose sensitivity to sub-solar stars, except above the turnoff. This will be important to consider when computing our sensitivity to ejectees in Section 3. At solar metallicity, the isochrones straddle the color-index threshold in the region  $0.4 < (g - r)_0 < 0.6$ , deviating by an amount that is small compared to the 0.105 color-index threshold over the entire range. Hence, we obtain roughly 50% sensitivity to solar-metallicity G stars, at a cost of only about 1 fiber per plate, thus not substantially interfering with any other program. And, at higher metallicity, the recovered fraction is substantially higher.

### 3. Results

#### 3.1. Where are the Old-Population HVS?

The selection described above resulted in a total of 361 target stars within 181 SEGUE-2 fields. The velocity distribution of these targets is shown in Figure 2. As can be seen from the velocity distribution, while there are high-velocity objects, none of the targets is moving in excess of, nor even close to, Galactic escape speed (e.g., Xue et al. 2007). The selection therefore uncovered no metal-rich ejectees from this carefully constructed sample. Our null result may reflect a true dearth of old-population HVS in the halo, or it may reflect a target selection algorithm that is too stringent. In order to determine which is the case, we compute our sensitivity below.

#### 3.2. Sensitivity to Metal-Rich Ejectees

We begin with a simple order-of-magnitude estimate of our survey sensitivity. We first define what is meant by “sensitivity”. Consider a Galactocentric spherical shell of thickness  $\Delta r$ . A star moving with speed  $v$  out of the GC will spend a time  $\Delta t = (1000 \text{ km s}^{-1}/v) \times (\Delta r/1 \text{ kpc})$  Myr traversing the shell. The total sensitivity to objects at a given velocity is therefore the integral of this quantity over the survey magnitude range and volume probed including selection effects. For this initial example, consider targeting every star of a single stellar type, with absolute magnitude  $M_g = 4.5$ , to the survey limiting magnitude of  $g =$

20 over the full area of the SEGUE-2 survey. Such stars can be probed to distances of approximately  $d = 10^{0.2(g-M_g+5)} \text{pc} = 12.5 \text{kpc}$  from the Sun. Each SEGUE-2 spectroscopic plate has an area of  $\Omega_{plate} = 7 \text{deg}^2$ , and there are a total of  $N_{plates} = 181$ . The survey volume, as seen from the Sun, is therefore  $V_{probed,\odot} = N_{plate}\Omega_{plate}d^3/3 = 265 \text{kpc}^3$ . This corresponds to a *Galactocentric* shell thickness of  $\Delta r_{GC} = V_{probed,\odot}/4\pi d_g^2$ , where  $d_g$  is the corresponding Galactocentric distance of the survey limit. At a fixed velocity, we can compute the time an ejectee spends in this shell, and therefore, the sensitivity as defined above. For a fiducial survey direction in which  $d_g$  corresponds to 10 kpc, and a fiducial velocity of  $500 \text{km s}^{-1}$ , the star spends a total of 0.42 Myr traversing the shell, and the survey would be sensitive to stars of this type if they were ejected at a rate of  $\sim 2.3 \text{Myr}^{-1}$ .

To compute the true survey sensitivity, we begin by fixing the absolute magnitude at a range of values (as above), and also consider a continuous range of ejection energies (parameterized by the HVS velocity at the time it passes the solar circle). For each of the SEGUE-2 plates and for each apparent magnitude in our selection interval, we compute  $d$ ,  $d_g$ , and the local velocity, and then simulate measurement of the star, allowing for proper-motion errors. The resulting “measurements” are then fed into the same algorithm that was used to select HVS candidates. Summation over all fields and apparent-magnitude intervals then yields the total sensitivity (in Myr). We note the sharp contrast in character between our completeness corrections and those made by Kollmeier et al. (2009). That sample, although huge in an absolute sense, contained only a small fraction of potential HVS stars because it was not pre-selected. Hence there was a large completeness penalty. The present sample has stringent selection, so that the only completeness factors are those due to photometric errors (which scatter HVS in and out of our selection box) and the SEGUE-2 proper-motion-error completeness factor of 0.87. Hence, our completeness factor (computed rigorously within our code) is of order 50%. The result is shown in Figure 3. At  $M_g = 4.5$  and  $v_{\odot} = 500 \text{km s}^{-1}$ , the sensitivity is 0.16 Myr, consistent (within a factor of 3) with our order of magnitude calculation.

Finally, to determine the sensitivity of the survey, we integrate the functions shown in Figure 3 over isochrones (An et al. 2009) of various ages and metallicities. That is, at each mass step (covering  $\Delta \log m$ ), with specified  $g - r$  color and  $ugr$  color index, we multiply  $\Delta \log m$  by the value indicated in Figure 3 and by the fraction of stars that survive our color selection (given the photometric errors), and sum over the entire isochrone. This yields a sensitivity  $S$  (in Myr-dex). We therefore compute our sensitivity for isochrones of fixed age and a range of mass. Since we detected no HVS in our survey, we have  $1 - e^{-n}n^0/n! \rightarrow 95\%$  confidence that there are fewer than  $n = 3$  expected detections over the range of mass and age to which we are sensitive. That is, we obtain a lower limit  $\Gamma > 3S^{-1}$ , where  $\Gamma$  is the rate of HVS ejections per Myr per dex. In Figure 4 we plot this lower limit on  $\Gamma$  as a function of

population age for a range of metallicities at a fixed velocity at the solar circle of  $500 \text{ km s}^{-1}$ . As can be seen from the figure, our strongest limits apply to super-solar metallicity stars with ages between 3-5 Gyr. For comparison, we also show the rate derived from the Brown et al. (2009) survey, which is sensitive to stars of ages of roughly 150 Myr. Rather than limits, that survey has secure detections, so we plot it as a single point in the diagram. However, it is clear from this figure that our survey probes a very different set of stellar parameters relative to Brown et al. (2009).

### 3.3. Limits on Metal-Rich Ejectees

Our survey uncovered no metal-rich hypervelocity stars. As we have just demonstrated, our well-defined selection allows us to convert this null detection into an upper limit on the ejection rate as a function of stellar type. In Figure 5, we show our ejection limits as a function of velocity at the solar circle for several population ages and metallicities. We also show for comparison the results of the Brown et al. (2009) survey over the velocity range these HVS were observed. At sub-solar metallicities, our limits are no more constraining than the K09 results (slightly less stringent in fact; K09 found that there can be at most 100 times the ejection of old-population stars as young population stars and we find a limit of 120). However, at solar metallicity and above, our limits are significantly stronger. For these stars, there can be no more than a factor of 30 times more solar-metallicity, low-mass stars relative to B-star ejectees.

At  $\sim 500 \text{ km s}^{-1}$  our limit on the ejection of solar-metallicity stars from Figure 5 is roughly  $\Gamma^{5\text{Gyr},\text{solar}} < 410(\text{Myr} - \text{dex})^{-1}$ . At  $[\text{Fe}/\text{H}] = +0.2$ , our limits are improved to  $\Gamma^{5\text{Gyr},\text{super-solar}} < 175(\text{Myr} - \text{dex})^{-1}$ .

### 3.4. Comparison to Young HVS

The Brown et al. (2009) sample has 14 detected HVS objects over a total survey area  $\Delta\Omega = 5000 \text{ deg}^2$ , which corresponds to an ejection rate of roughly  $1.75 \text{ Myr}^{-1}$  over a mass range of roughly  $3-4M_{\odot}$  (0.12 dex), or  $\Gamma^{100\text{Myr}} = 14(\text{Myr} - \text{dex})^{-1}$ . For a Salpeter mass function with shape  $dN/d\log M \propto M^{-1.35}$ , we naively expect a factor of 5 more stars per dex at  $1M_{\odot}$  compared to  $3.5M_{\odot}$  available at the GC for ejection. Of critical importance, however, is the relative lifetimes of these two populations. Our sensitivity is maximized to stars of ages 5 Gyr. The Brown et al. (2009) survey is targeted for stars with lifetimes of roughly 150 Myr. Therefore we must consider this additional factor of *33 times* more

stars available for ejection, were they in fact accumulating at the GC for 5 Gyr. Therefore, provided the mass function is roughly Salpeter at the GC and that stars were accumulating for at least 5 Gyr, there should be  $\sim 165$  times more old-population stars (which our survey targets) relative to B-stars available for ejection. Our limits place the ejection rate at no more than  $\sim 30$  times more old-population ejectees relative to the known population of young ejectees. These stars are either not present at the GC, they have sub-solar metallicity, or the ejection mechanism quite strongly prefers high-mass stars at high velocity, by a factor of roughly 5.5.

#### 4. Discussion and Conclusions

We have implemented a well-defined target selection algorithm within the SEGUE-2 survey to search for metal-rich old-population hypervelocity stars. We targeted over 300 stars and found no hypervelocity stars. This null result allows us to place new limits on the ejection of metal-rich old-population HVS from the GC as a function of mass, metallicity, velocity, and population age. Our results imply that either the mass function at the GC is top-heavy, or the mechanism for ejection of HVS significantly favors massive stars at the level of 1:5.5, or that the stars being ejected from the GC are sub-solar metallicity.

It is certainly plausible that the ejection mechanism favors high-mass stars, or more precisely, ejects low-mass stars at velocities too low to be detected by our survey. It is possible that low-mass stars are being ejected at velocities below our survey threshold of  $400 \text{ km s}^{-1}$ , and some mechanisms, e.g., Hills (1988), would predict that low mass binaries would be ejected at lower velocity. Indeed, detailed calculations by Kenyon et al. (2008) show that at  $1M_{\odot}$ , the predicted velocity distribution at  $400 \text{ km s}^{-1}$  is strongly suppressed relative to more massive stars – our result in Figure 2 can be quantitatively compared to their predicted radial velocity distribution to determine whether the observations are consistent with the predictions for *bound* ejectees. Furthermore, high-mass stars are thought to have a binary fraction near unity (Pinsonneault & Stanek 2006). The binary fraction is indeed observed to be substantially less than unity at lower mass in the solar neighborhood (Duquennoy & Mayor 1991; Lada 2006), and it is possible that conditions at the GC result in a similar F/G binary fraction. Therefore, the classic binary disruption mechanism could very well favor high-mass stars in this scenario. Relaxing the assumption of a universal mass function, however, it is also possible that there are simply very few old stars at the GC. For example, Perets et al. (2007) demonstrate that, for reasonable assumptions about the mass function and old-star binary-fraction, the ejection rate of  $1M_{\odot}$  stars should be approximately  $5 \times 10^{-7} \text{ yr}^{-1}$  (but see Yu & Tremaine 2003), and could be substantially enhanced by the

presence of a secondary massive perturber as envisioned by e.g., Polnarev & Rees (1994), Baumgardt et al. (2006), and Levin (2006) and not included in the Kenyon et al. (2008) calculations.

One mechanism that has been suggested is that the HVS have nothing at all to do with the black hole at the GC and the dynamics there, but rather they reflect debris of a satellite with pericenter close to the GC (Abadi et al. 2009) and a large population of young stars. The anisotropy of the known HVS potentially supports this interpretation. A satellite galaxy would have the normal complement of old-population stars compared to young stars, and that would show up in our limits. While we do not see these stars, if the satellite system had low metallicity similar to the current satellites of the Milky Way, it would not be detectable in our survey. It is also possible that our SEGUE-2 pointings were not sufficiently aligned with the proposed direction of this debris.

The new limits derived here, in conjunction with the known HVS detections at higher mass, provide an important constraint on models of HVS ejection. The target strategy implemented here represents an efficient and economical way to probe low mass populations ejected from the GC at modest spectroscopic follow-up cost. Future spectroscopic surveys with similarly stringent target selection could strengthen these limits. Deciphering the true distribution of GC ejectees as a function of mass, age, velocity, and position will continue to provide valuable insight into the still obscure Galactic center.

JAK acknowledges the hospitality and support of the KITP during the program “Building the Milky Way” which was funded by NSF grant PHY-0551164. Work by A.G. was supported in part by NSF grant AST-0757888. Work by H.M. was supported in part by NSF grant AST-0098435. T.C.B. and Y.S.L. acknowledge partial funding of this work from grants PHY 02-16783 and PHY 08-22648: Physics Frontier Center/Joint Institute for Nuclear Astrophysics (JINA), awarded by the U.S. National Science Foundation. Funding for SDSS-III has been provided by the Alfred P. Sloan Foundation, the Participating Institutions, the National Science Foundation, and the U.S. Department of Energy. The SDSS-III web site is <http://www.sdss3.org/>. SDSS-III is managed by the Astrophysical Research Consortium for the Participating Institutions of the SDSS-III Collaboration including the University of Arizona, the Brazilian Participation Group, Brookhaven National Laboratory, University of Cambridge, University of Florida, the French Participation Group, the German Participation Group, the Instituto de Astrofísica de Canarias, the Michigan State/Notre Dame/JINA Participation Group, Johns Hopkins University, Lawrence Berkeley National Laboratory, Max Planck Institute for Astrophysics, New Mexico State University, New York University, the Ohio State University, University of Portsmouth, Princeton University, University of Tokyo, the University of Utah, Vanderbilt University, University of Virginia, University of

Washington, and Yale University.

## REFERENCES

- Abazajian, K., et al., 2003, *AJ*, 126, 2081
- Abazajian, K., et al., 2004, *AJ*, 128, 502
- Abazajian, K., et al., 2005, *AJ*, 129, 1755
- Abazajian, K., et al., 2009, *ApJS*, 182, 543
- Abadi, M. G., Navarro, J. F., & Steinmetz, M. 2009, *ApJ*, 691, L63
- Adelman-McCarthy, J. K., et al., 2006, *ApJS*, 162, 38
- Adelman-McCarthy, J. K., et al., 2007, *ApJS*, 172, 634
- Adelman-McCarthy, J. K., et al., 2008, *ApJS*, 175, 297
- Allende Prieto, C., et al. 2008, *AJ*, 136, 2070
- An, D., et al. 2009, *ApJ*, 700, 523
- Baumgardt, H., Gualandris, A., & Portegies Zwart, S. 2006, *MNRAS*, 372, 174
- Brown, W. R., Geller, M. J., Kenyon, S. J., & Kurtz, M. J. 2005, *ApJ*, 622, L33
- Brown, W. R., Geller, M. J., Kenyon, S. J., Kurtz, M. J., & Bromley, B. C. , 2007a, *ApJ*, 660, 311
- Brown, W. R., Geller, M. J., Kenyon, S. J., Kurtz, M. J., & Bromley, B. C. 2007b, *ApJ*, 671, 1708
- Brown, W. R., Geller, M. J., & Kenyon, S. J., 2009, *ApJ*, 690, L69
- Duquenois, A., & Mayor, M. 1991, *A&A*, 248, 485
- Edelmann, H., Napiwotzki, R., Heber, U., Christlieb, N., & Reimers, D. 2005, *ApJ*, 634, L181
- Fukugita, M., Ichikawa, T., Gunn, J. E., Doi, M., Shimasaku, K., & Schneider, D. P., 1996, *AJ*, 111, 1748

- Gould, A., & Kollmeier, J. A. 2004, *ApJS*, 152, 103
- Gunn, J. E., et al., 1998, *AJ*, 116, 3040
- Gunn, J. E., et al., 2006, *AJ*, 131, 2332
- Hills, J. G. 1988, *Nature*, 331, 687
- Hirsch, H. A., Heber, U., O’Toole, S. J., & Bresolin, F. 2005, *A&A*, 444, L61
- Hogg, D. W., Finkbeiner, D. P., Schlegel, D. J., & Gunn, J. E. 2001, *AJ*, 122, 2129
- Ivezić, Ž, et al., 2004, *Astronomische Nachrichten*, 325, 583
- Kenyon, S. J., Bromley, B. C., Geller, M. J., & Brown, W. R. 2008, *ApJ*, 680, 312
- Kollmeier, J.A.. & Gould, A., 2007, *ApJ*664, 343
- Kollmeier, J. A., Gould, A., Knapp, G., & Beers, T. C. 2009, *ApJ*, 697, 1543
- Lada, C. J. 2006, *ApJ*, 640, L63
- Lee, Y. S., et al. 2008a, *AJ*, 136, 2022
- Lee, Y. S., et al. 2008b, *AJ*, 136, 2050
- Levin, Y. 2006, *ApJ*, 653, 1203
- Lupton, R., et al., 2001, in *ASP Conf. Ser. 238, Astronomical Data Analysis Software and Systems X*, ed. F. R. Harnden, Jr., F. A. Primini, and H. E. Payne (San Francisco: Astr. Soc. Pac.) p. 269
- Munn, J.A., et al. 2004, *AJ*, 127, 3034
- Perets, H. B., Hopman, C., & Alexander, T. 2007, *ApJ*, 656, 709
- Pinsonneault, M. H., & Stanek, K. Z. 2006, *ApJ*, 639, L67
- Polnarev, A. G., & Rees, M. J. 1994, *A&A*, 283, 301
- Smith, J. A., et al. 2002, *AJ*, 123, 2121
- Stoughton, C. et al., 2002, *AJ*, 123, 485
- Tucker, D., et al. 2006, *Astronomische Nachrichten*, 327, 821
- Yanny, B. et al. 2009, *AJ*, 137, 4377

Yu, Q., & Tremaine, S. 2003, ApJ, 599, 1129

York, D. G., et al., 2000, AJ, 120, 1579

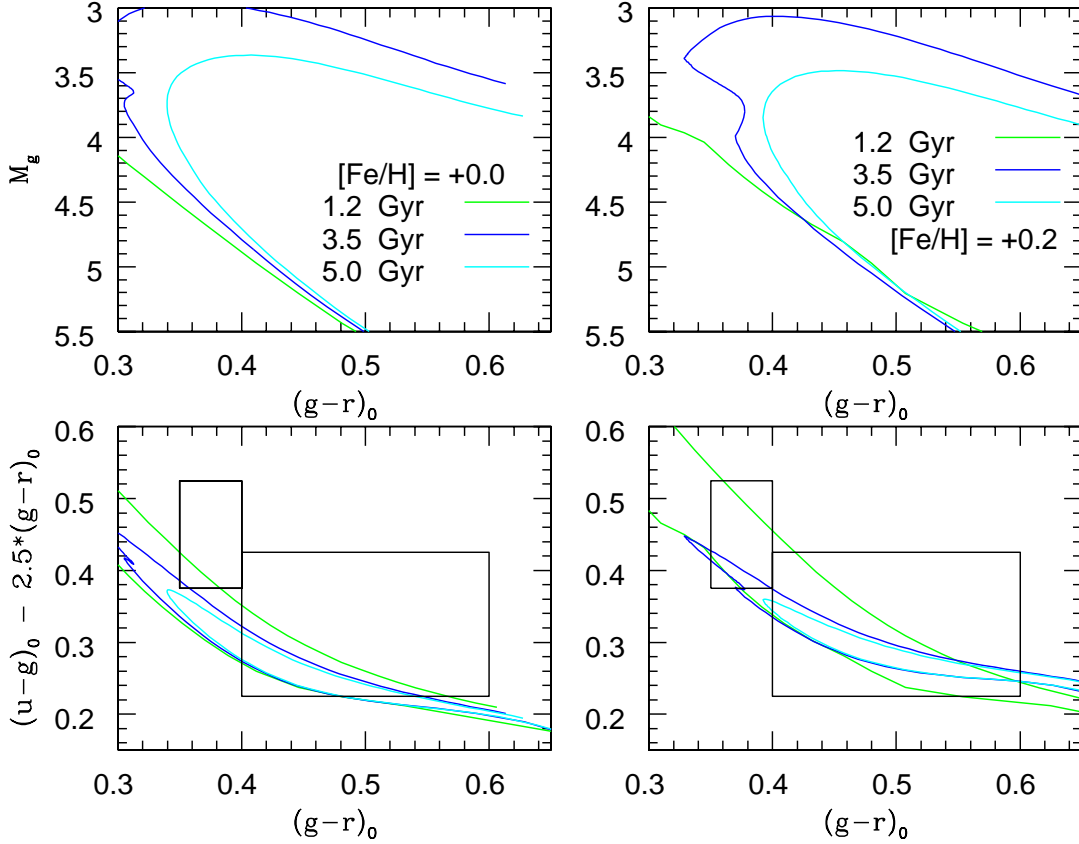


Fig. 1.— Color-magnitude and color-index diagram for theoretical isochrones computed by An et al. (2009) as a function of age and metallicity. Left panels show results for a  $[\text{Fe}/\text{H}]=0.0$  isochrone; right panels show a  $[\text{Fe}/\text{H}]=+0.2$  isochrone. Colors green, blue, and cyan show ages of isochrones corresponding to 1.2, 3.5, and 5.0 Gyr, respectively. Our color selection boxes are superposed on the isochrones in the lower panels as black rectangles. Our survey has sensitivity to solar and super-solar metallicity stars.

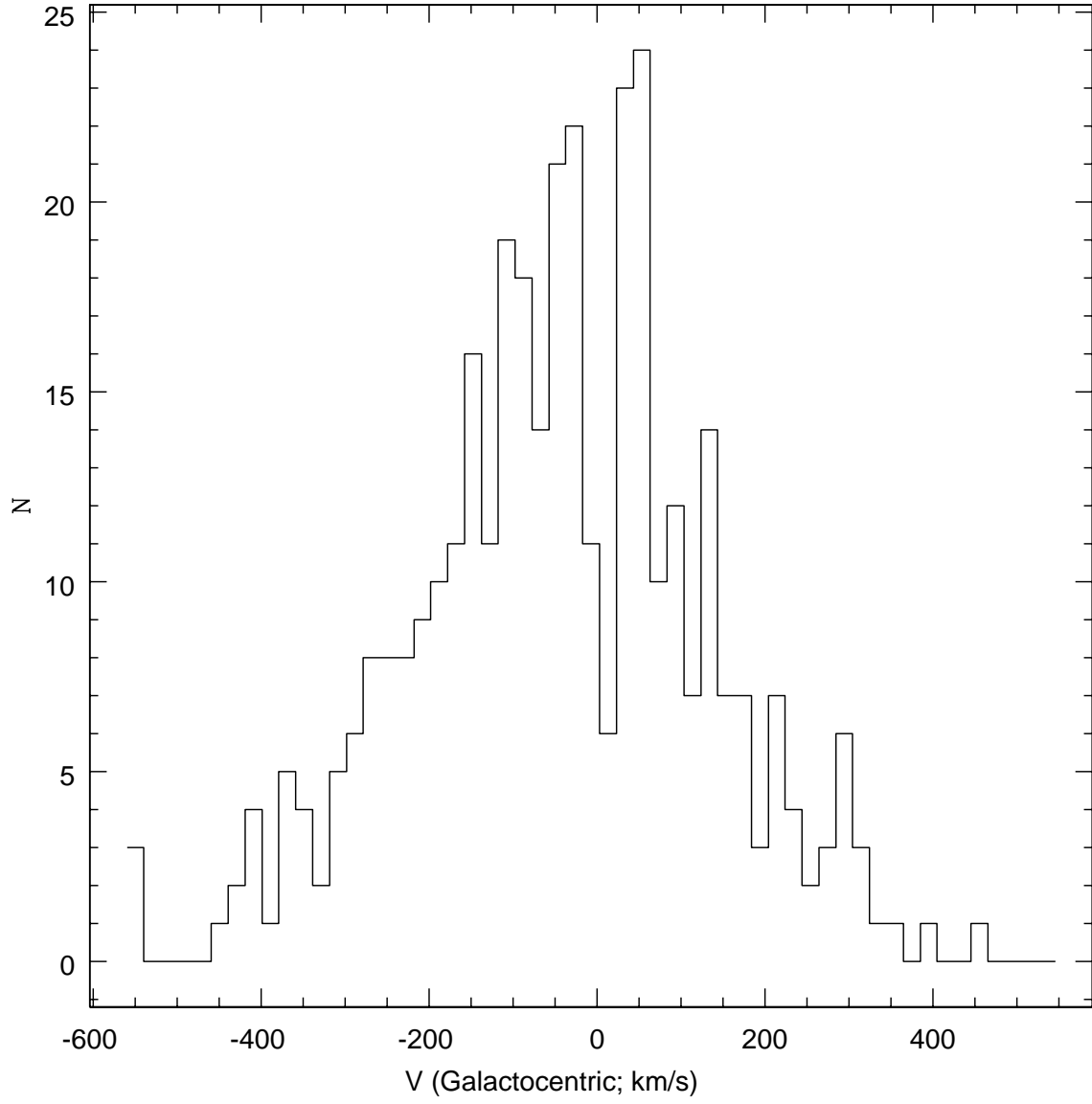


Fig. 2.— Galactocentric velocity distribution of HVS targets from SEGUE-2.

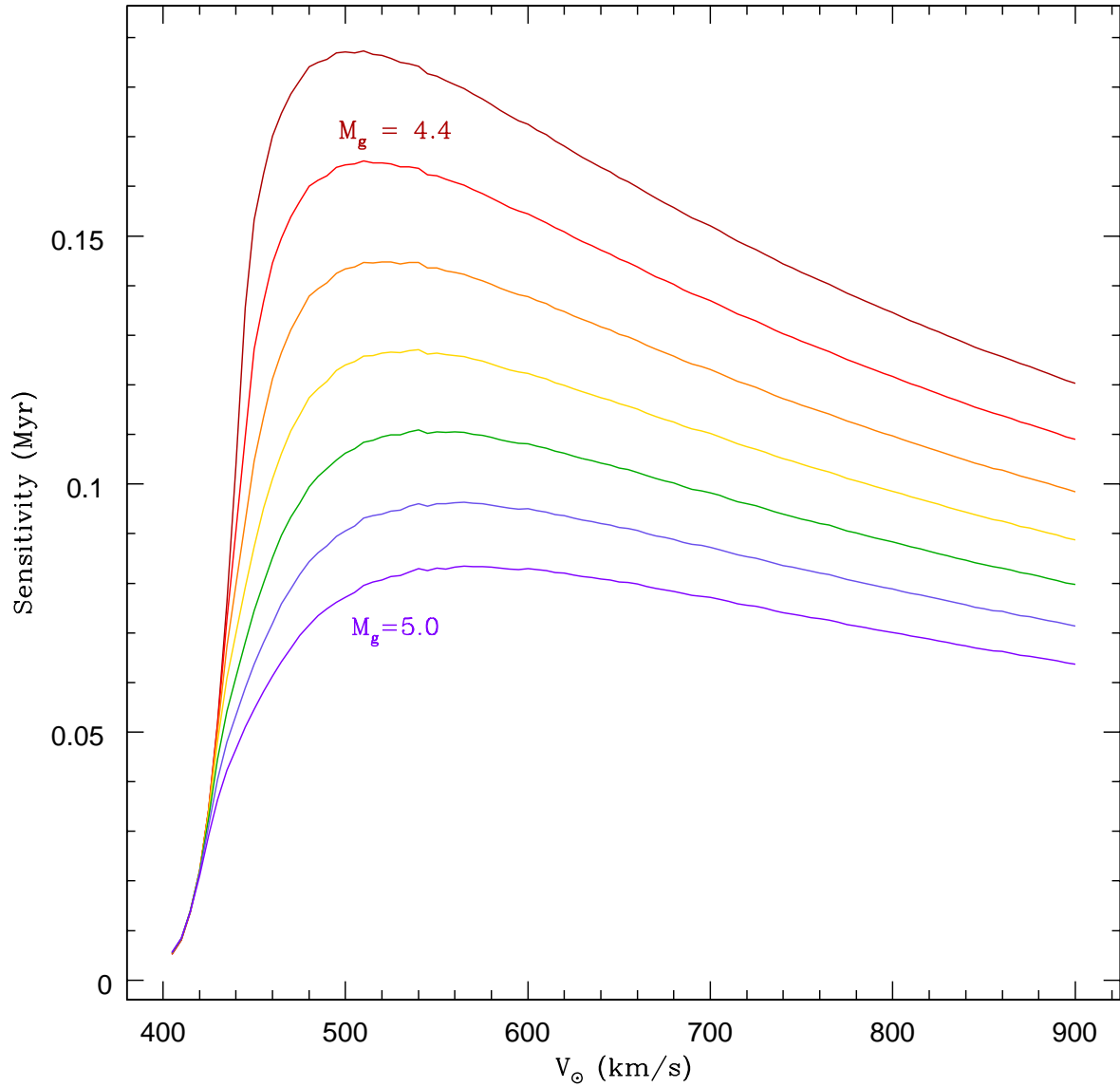


Fig. 3.— Sensitivity to HVS as a function of velocity at the solar circle and absolute magnitude of stellar population. Curves from top to bottom show our sensitivity as a function of absolute magnitude ranging from  $M_g = 4.4$  (top) to  $M_g = 5.0$  (bottom) in increments of 0.1 magnitudes.

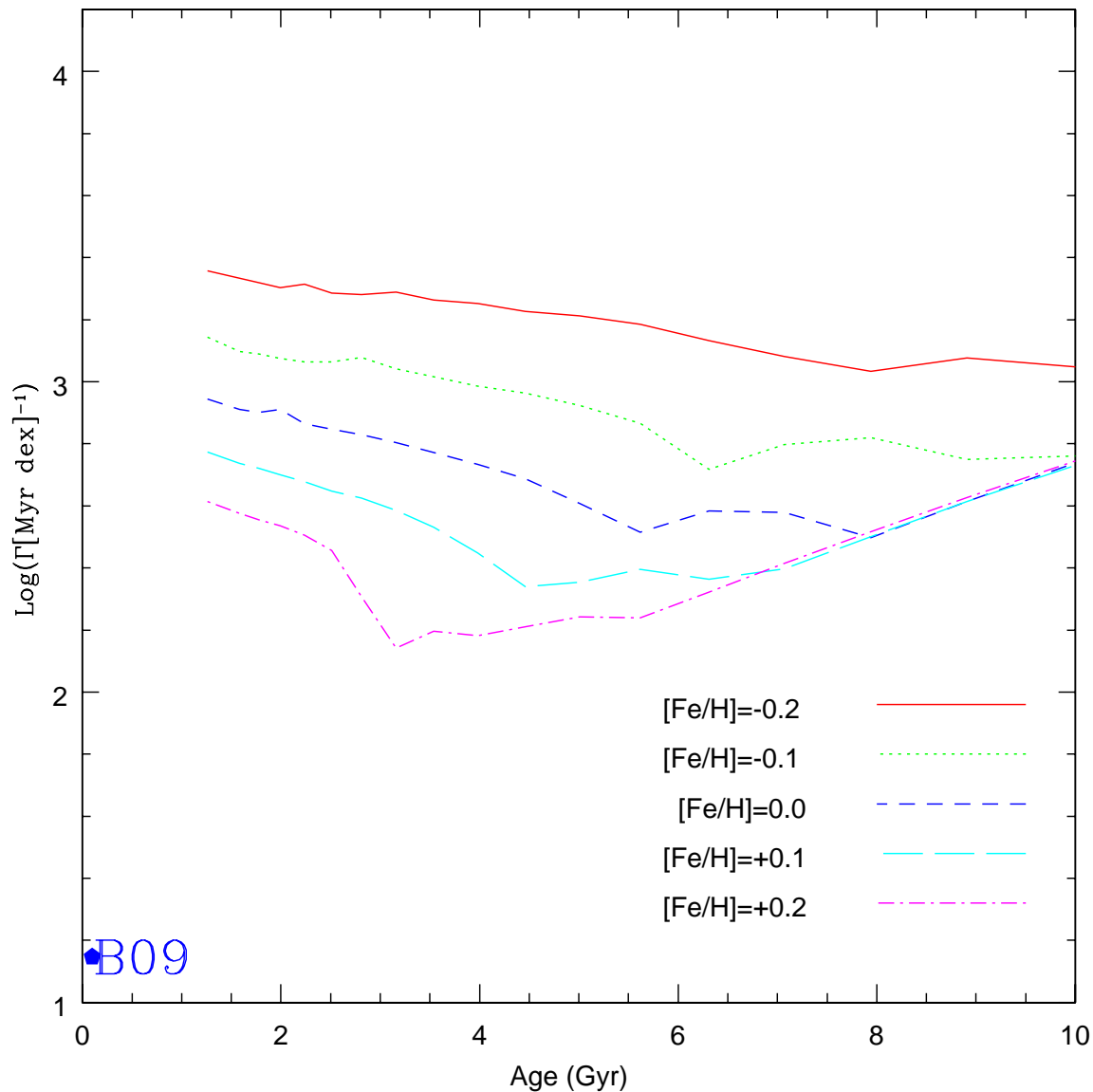


Fig. 4.— Limits on the ejection of old-population HVS as a function of metallicity and age, for velocities at the solar circle  $v_{\odot} = 500 \text{ km s}^{-1}$ . Solid, dotted, short-dashed, long-dashed, and dot-dashed lines correspond to metallicities of  $[\text{Fe}/\text{H}] = +0.2, +0.1, 0.0, -0.1,$  and  $-0.2$ , respectively. For comparison, we show the Brown et al. (2009) survey results, which probe a very different age regime compared to our survey. Our ejection limits are most stringent for metal-rich stars; our sensitivity to sub-solar metallicity is significantly degraded.

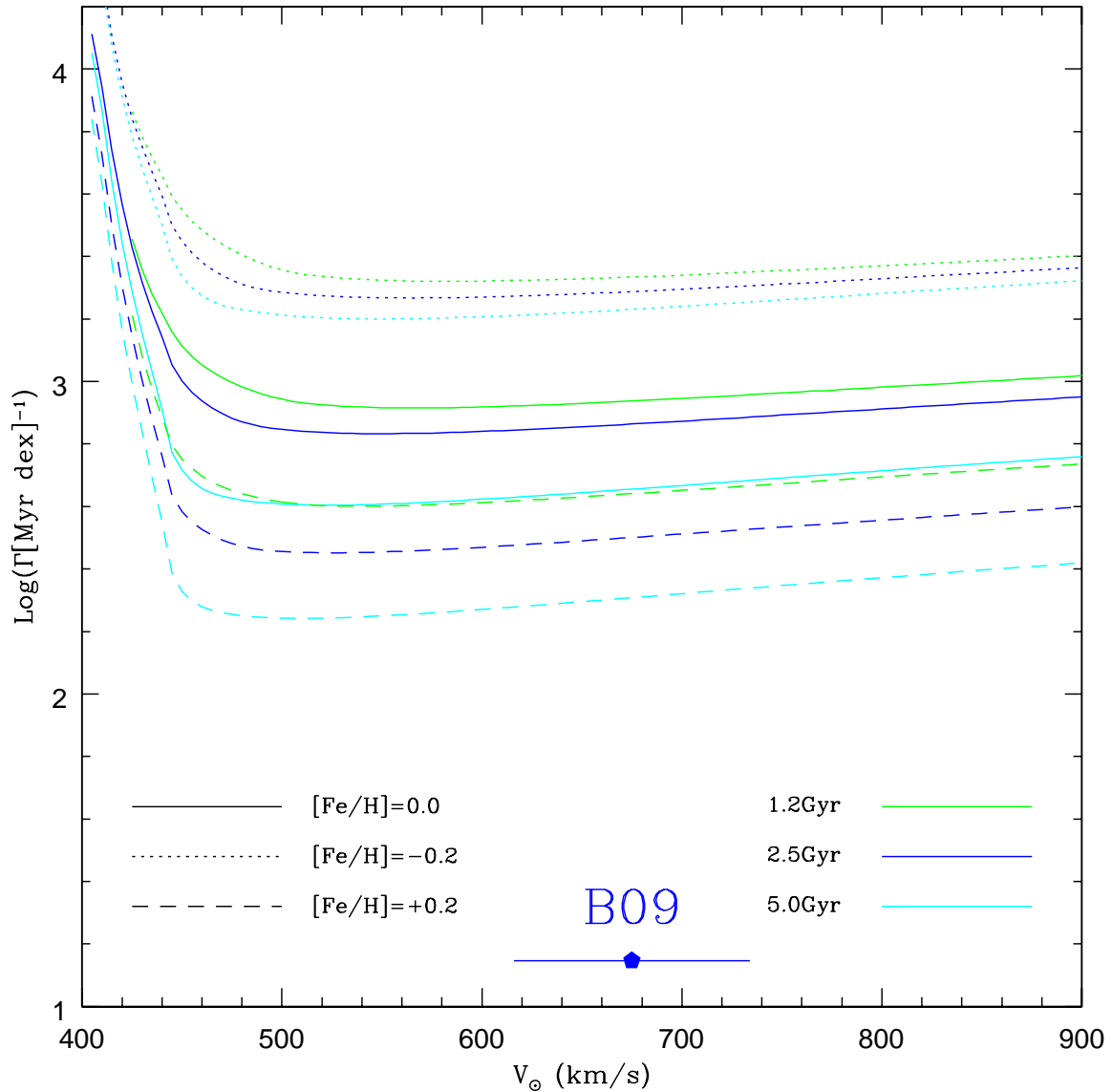


Fig. 5.— Limits on the ejection of old-population HVS as a function of metallicity, age, and velocity. Solid, dotted, dashed lines correspond to metallicities of  $[\text{Fe}/\text{H}]=0.0$ ,  $-0.2$  and  $+0.2$ , respectively. Colored lines show different population ages of green, blue, cyan to 1.2, 2.5 and 5.0 Gyr, respectively. Each point of the solid curves is formed by integrating over a set of corresponding points at the same velocity in Figure 3, weighting by the fraction that survive the color selection for each isochrone, and dividing 3 by the result. For comparison, we show the Brown et al. (2009) survey results.